# Indole-3-acetic acid promotes growth in bloom-forming cyanobacteria via a potential antioxidant response

Hunter R. Baylous[1#], Matthew F. Gladfelter[2#], Malia I. Gardner[1], Madalynn Foley[1], Alan E. Wilson[2], Morgan M. Steffen[1*]

1. James Madison University, Harrisonburg, VA USA 22801
2. Auburn University, Auburn, AL USA 36849

* Corresponding author steffemm@jmu.edu

# The authors contributed equally to this work

Insert ORCID:

HRB

MFG

MIG

MF

AEW

MMS https://orcid.org/0000-0001-9755-9879

**Abstract**

Interactions between bacteria and algae in the phycosphere constrain biogeochemical cycling in aquatic ecosystems. Here, we explore the impact of one chemical currency exchanged between bacteria and their photosynthetic hosts in both the phycosphere and the rhizosphere, indole-3-acetic acid (IAA). Exposure to IAA and its precursor tryptophan resulted in a strong growth response in a bloom of the freshwater cyanobacterium *Microcystis*. Metatranscriptome analysis revealed the induction of an antioxidant response in *Microcystis* upon exposure to IAA, potentially allowing populations to increase photosynthetic rate and overcome internally generated reactive oxygen. Our data reveal that co-occurring bacteria within the phycosphere microbiome exhibit a division of labor for supportive functions such as nutrient mineralization and transport, vitamin synthesis, and reactive oxygen neutralization. These complex dynamics within the *Microcystis* phycosphere microbiome are an example of interactions within a microenvironment that can have ecosystem-scale consequences.

## Introduction

Freshwater ecosystems are considered sentinels of global disturbance. One destructive symptom of disturbance to lakes is the dysbiosis of ecosystem microbiomes, shifting freshwater microbial communities toward organisms such as bloom-forming cyanobacteria. Dominance of cyanobacteria can disrupt normal ecosystem function, driving elevated pH[1–3], anoxic conditions[4,5], and toxin exposure[6–8]. Often, the ecosystem damage associated with accumulation of cyanobacterial biomass is due to the activity of co-occurring heterotrophic bacteria, which can degrade cyanobacterial biomass and subsequently drive anoxic conditions. Interactions between cyanobacteria and heterotrophic bacteria occur in the phycosphere, a microenvironment surrounding phytoplankton cells analogous to the rhizosphere of plants. While largely overlooked for several decades, the exchange of chemical currencies between algae and their phycosphere constituents is now recognized as a key contributing factor to aquatic ecosystem dynamics and the occurrence symptoms of dysbiosis such as harmful algal blooms (HABs)[9,10].

Interactions in the phycosphere support phytoplankton growth through the exchange of nutrients such as nitrogen and phosphorus[9,11–13], production of enzymes that neutralize reactive oxygen[14,15], and vitamins and other hormones[16–18]. In turn, phytoplankton provide organic carbon to the bacterial constituents of the phycosphere. While considerable work has been done to understand phycosphere dynamics of marine eukaryotic algae[9,19,20], less is known about the interactions that occur between freshwater cyanobacteria and their associated phycosphere microbiome. Here, we report the impact and potential mechanism of growth promotion by the hormone indole-

3-acetic acid (IAA) in the phycosphere of the cyanobacterium *Microcystis*. *Microcystis* spp. are globally pervasive cyanobacteria that form destructive blooms in both freshwater and brackish systems[21–23]. Using time-series metatranscriptomics, we found that IAA exposure triggers an antioxidant response by *Microcystis* during bloom conditions. This molecular response was accompanied by an increase in growth rate in the *Microcystis* population. Within the bacterial population, we found evidence for clear division of labor between individual bacterial genera that fill individual functional roles within the phycosphere of this globally pervasive freshwater cyanobacterium. These observations indicate that dynamics within the phycosphere are both powerful and complex, with a single hormone able to amplify the dominance of a destructive cyanobacterium in a freshwater system.

## Results and discussion

**Bloom geochemistry.** Samples were collected across the time series from each mesocosm for nutrient, toxin, and pigment analyses. Mesocosm incubations were conducted over a 7 day time series during a *Microcystis* bloom in the S-10 experimental pond at Auburn University (Fig. 1a). Water temperature varied by ~3.5 °C throughout the experiment, peaking at the 0 h time point at 24.3 °C and steadily decreasing to 20.9 °C at the 7 day time point (Supplementary Table 1). Notably, TN concentrations were elevated in the tryptophan treatments throughout the experiment, driving them to P deficiency between 2 h and 48 h (Fig. 1b). Dissolved oxygen ranged from 7.41 - 12.78 mg/L, and conductivity ranged from 68.5 - 104.1 µS/cm (Supplementary Table 1). The pH during the incubation period ranged from 8.13 - 10.31, indicating that the pH conditions of the blooms were basic, although this is common for bloom conditions

70 (Supplementary Table 1)[2,3]. Both chlorophyll (chl) *a* and phycocyanin concentrations
71 were measured throughout the experiment, with phycocyanin concentrations peaking at
72 the 12 h time point for each treatment, while chl *a* concentrations remained relatively
73 steady throughout the 7 d incubation (Fig. 1c). Microcystin concentrations were
74 measured at the start and end of the experiment, with toxin levels decreasing
75 significantly ($p<0.03$) in across all treatments over the course of the experiment (Fig.
76 1d). Decreasing toxin corresponds to the relatively low expression of the *mcy* cassette
77 throughout the course of the experiment (Fig. 2b).

78 **Response of *Microcystis* to IAA exposure.** The impact of treatment with both IAA and
79 tryptophan on the growth of *Microcystis* was immediate, with significant changes in cell
80 abundance observed at nearly all time points compared to the control ($p<0.05$; Fig. 2a).
81 Maximum growth rate was also significantly increased for both the tryptophan and IAA
82 treatments compared to the control ($p<0.01$; Table 1). To validate these observations in
83 pond S-10, we repeated the incubation conditions in a small retention pond on the
84 James Madison University campus and with non-axenic cultures of *M. aeruginosa*
85 CCMP 3462 and observed similar significant differences in maximum growth rate in
86 these two distinct systems, indicating the growth impact of IAA and its amino precursor
87 across multiple strains of *Microcystis* and in variable growth conditions (Table 1).

88 To determine the molecular mechanisms driving this obvious growth impact of IAA and
89 tryptophan, we generated metatranscriptomes from biomass collected at 0, 2, and 24
90 hours. Global expression patterns across the *Microcystis* genome suggested that
91 expression was driven primarily by time point, and directed analysis of only those genes
92 that were differentially expressed shows a similar clustering pattern (Fig. 2a;

93 Supplementary Fig. 1). We compared expression profiles for each treatment across the
94 time series to identify the impact of incubation with tryptophan and IAA on the
95 interactions within the *Microcystis* bloom microbiome (Fig. 2a). At 2 hours, 91 genes
96 were significantly differentially expressed in the IAA treatment and 48 in the tryptophan
97 treatment, exclusive of those genes that were also significantly differentially expressed
98 in the control treatment (Fig. 2a; Supplementary Fig. 2). Exclusion of those genes that
99 were significantly different across the time series in the control treatment ensured that
100 only those genes that were influenced by treatment with IAA or tryptophan were
101 considered. The greatest number of genes were significantly differentially expressed at
102 12 hours, confirming the impact of diel cycling on *Microcystis* expression (Fig. 2a;
103 Supplementary Fig. 2)[24]. In the IAA treatment, 916 genes were differentially regulated,
104 and 322 of those genes were uniquely differentially regulated compared to the control
105 treatment (Supplementary Fig. 2). Compared to the control and tryptophan treatments,
106 the IAA treatment had the greatest number of genes that were exclusively differentially
107 regulated, 105 upregulated and 140 downregulated, respectively (Supplementary Fig.
108 2). This differential regulation indicates that while time point primarily drove the
109 expression response, exposure to IAA resulted in unique changes to *Microcystis*
110 molecular physiology. By 24 hours, 220 genes in the IAA treatment and 59 genes in the
111 tryptophan treatment were differentially expressed, excluding the control
112 (Supplementary Fig. 2; Fig. 2a).

113 While microcystin concentrations declined over the 7 day time series, multiple genes in
114 the *mcy* gene cassette were significantly upregulated at 12 hours in the IAA (*mcyD,*
115 *mcyG*) and tryptophan (*mcyD*) treatments (Fig. 2b; 2c). There is a noted lag in toxin

116 production compared to mcy gene expression changes, and overall expression of the
117 *mcy* cassette was low relative to overall gene expression[25]. However, the potential for
118 IAA to influence toxicity of *Microcystis* bloom populations warrants further exploration.

119 Incubation with IAA or tryptophan had a significant impact on genes involved in nutrient
120 acquisition and metabolism, with the greatest impact on the expression of genes related
121 to nitrogen and sulfur metabolism. The gene encoding cyanase, which degrades urea
122 and produces $NH_4^+$, was upregulated at 12 hours in both IAA and tryptophan treatments
123 (Fig. 3a). This enzyme is a potential marker for urea utilization and its upregulation may
124 indicate use of urea at 12 hours by *Microcystis* populations in the amended
125 treatments[26]. However, transport of urea, ammonium, and nitrate were all
126 downregulated during the time series. Urea transporter *urtB* was downregulated at 24
127 hours in both the IAA and tryptophan treatments. Ammonium transport (MAE_RS17310)
128 was exclusively downregulated in the IAA treatment at 24 hours, while nitrate transport
129 was downregulated at 12 hours (MAE_RS06500, MAE_RS06505) in both treatments
130 and 24 hours (*ntrB1*, MAE_RS6505) in the tryptophan treatment (Fig. 3a). Both
131 tryptophan and IAA contain nitrogen and could serve as nitrogen sources, although
132 *Microcystis* does not have the full *iac* gene cassette that encodes degradation of IAA
133 and likely relies on the constituents of its microbiome for this service[27,28]. Sulfate
134 transporters *cysW* and *cysT* were upregulated at 2 hours, and *cysT* and MAE_RS13665
135 were upregulated at 24 hours in the IAA treatment (Fig. 3a). The sulfate permease *sulP*
136 was upregulated at 12 hours in the IAA treatment (Fig. 3a). The upregulation of these
137 genes is likely related to an increasing cellular demand for sulfur for cells treated with
138 IAA[29]. Cyanobacterial cells incorporate assimilated sulfur into cellular components

139 related to amino acids, photosynthesis, and other cellular processes. *cysK*, which
140 encodes cysteine synthase, was upregulated in both IAA and tryptophan treatments at
141 12 hours and may have been partly responsible for the increased sulfate demand (Fig.
142 3a).

143 Genes related to photosynthesis were broadly upregulated in response to IAA and/or
144 tryptophan addition. At 2 hours, *psbA1, 2, 3*, and *5* were upregulated in response to IAA
145 (Fig. 3b). At 12 hours, *psaA, psaB, psaC*, MAE_RS04200, MAE_RS10360, and
146 MAE_RS18960, all of which are implicated in photosystem function, were upregulated
147 in either the IAA or both IAA and tryptophan treatments (Fig. 3b). By 24 hours these
148 genes were no longer differentially regulated, indicating changes to photosynthetic
149 activity are an early response to IAA exposure, which has a substantial physiological
150 impact on photosynthetic machinery and may in turn explain increased demand for
151 nutrients such as sulfate. This increase in expression of genes related to photosynthesis
152 is likely related to the increase in cell density and growth rate observed after exposure
153 to IAA and tryptophan. Furthermore, these genes have demonstrated decreased
154 transcription under stress conditions[30], which are likely alleviated upon exposure to
155 IAA[31].

156 **IAA exposure induces antioxidant activity in *Microcystis*.** In the rhizosphere of
157 plants, bacterial-derived IAA serves to alleviate both biotic and abiotic stressors[32], and
158 preliminary evidence indicates IAA fills an equivalent role in the phycosphere of green
159 algae and *Microcystis*[31]. Auxins activate antioxidant defense systems in the green algae
160 *Chlorella vulgaris, Scenedesmus obliquus,* and *Acutodesmus obliquus*[31,33,34]*.* Incubation
161 of *C. vulgaris* cultures with exogenous IAA reduced $H_2O_2$ accumulation, stimulated the

162 antioxidant enzymes catalase, super oxide dismutase, and peroxidase, and induced
163 production of the antioxidants ascorbate and glutathione[33]. *Microcystis* possesses a
164 suite of genes that encode antioxidant enzymes, including thioredoxins, peroxidases,
165 super oxide dismutases, glutaredoxins, and peroxiredoxins, although catalase is notably
166 absent[14,35]. The antioxidant response to IAA exposure was immediate, with a
167 peroxiredoxin (MAE_RS15790) exhibiting significantly increased expression in the IAA
168 treatment at 2 hours (Fig. 3c). Multiple glutaredoxins (MAE_RS08180, *grxC2*) were
169 induced at 12 hours by the IAA treatment; *grxC* is induced under high light and $H_2O_2$
170 exposure in *Synechocystis*[36]. Thioredoxin-disulfide reductase (*trxB*) was upregulated in
171 the tryptophan treatment at 12 hours, and *trxA1*, which encodes a thioredoxin, was also
172 induced in both the IAA and tryptophan treatments at 12 hours (Fig. 3c). These proteins
173 are known components of the oxidative stress response of the freshwater cHAB
174 organisms *Microcystis* and *Dolichospermum*[37,38]. They have also been implicated in
175 microcystin toxin-mediated stress responses to ROS and nutrient depletion by
176 *Microcystis*[39]. Both thioredoxins and glutaredoxins contain the amino acid L-cysteine,
177 which may further explain the increased sulfur demand indicated by upregulation of
178 sulfate transporters.

179 By 24 hours, a suite of antioxidant enzymes, including peroxiredoxins (MAE_RS18020,
180 MAE_RS26595), glutathione peroxidase (MAE_RS27445), *trxB*, and sulfiredoxin
181 (MAE_RS17400) were upregulated in one or both treatments (Fig. 3c). Interestingly, a
182 thioredoxin (*trxA3*) and thioredoxin-dependent thiol peroxidase (*bcp*) were
183 downregulated in the IAA treatment at 12 and 24 hours, respectively. Induction of
184 different antioxidant related genes at different times in the tryptophan and IAA

185 treatments may be due to the lag in response in *Microcystis* when exposed to excess
186 tryptophan, as bacteria would need to synthesize IAA from the precursor prior to
187 inducing the antioxidant response.

188 Exposure to IAA changed *Microcystis* expression patterns in several sets of genes
189 implicated in general stress response (Fig. 3c). Multiple toxins from toxin-antitoxin pairs
190 related to stress response were downregulated at 2 (*vapC, relE*), 12 (*vapC*), and 24
191 hours (*vapC*). *vapC* arrests cell growth, while *relE* degrades RNA, resulting in cell death
192 or stasis[40–42]. At two hours, *recQ* (DNA repair), *pspA* (membrane stability), and
193 MAE_RS01465 and MAE_RS01475 (cell wall lysis) were all downregulated in both the
194 IAA and tryptophan treatments (Fig. 3c). Both *pspA* and *recQ* were also downregulated
195 at 12 hours in the IAA treatment, as were the chaperone *clpB*, metalloprotease *rseP*
196 (Fig. 3c). Stress markers *hemC, hemB2, dnaA, uvrB* were also downregulated at 24
197 hours (Fig. 3c). Overall, IAA may act to induce an antioxidant response and alleviate
198 other abiotic stressors, accompanied by an increase in cell density and growth rate.
199 This pattern of increased cell density, elongated log growth phase, induction of
200 antioxidants, and reduced abiotic stressors has been observed in both eukaryotic green
201 algae and rhizosphere microbiota. We hypothesize that antioxidant activity of bacterial-
202 derived IAA contributes to the ability of *Microcystis* to withstand internal ROS stress.

203 **Evidence for active bidirectional nutrient exchange in the *Microcystis***
204 **phycosphere during bloom conditions.** Of the ~1.5 billion reads analyzed, 29%
205 recruited to the genome of *M. aeruginosa* NIES 843, emphasizing the importance of
206 non-*Microcystis* organisms to the functional biodiversity of *Microcystis* blooms. The
207 percentage of reads recruited to *Microcystis* peaked at 2 hours and steadily declined

208 over the next two time points for all treatments (Fig. 4a). Total community abundance
209 based on assembled contigs validates the individual read recruitment, with
210 Proteobacteria and Cyanobacteria as the dominant bacteria phyla across all treatments
211 (Fig. 4b). Among the Cyanobacteria, *Microcystis* was the dominant genus across all
212 samples, representing 4.2 – 5.6% of assembled contigs (Fig. 4c). Within the non-
213 cyanobacterial population, three genera were the most abundant: *Cupriavidus*,
214 *Streptomyces*, and *Clostridium* (Fig. 4a; 4c). Notably, the presence of *Clostridium* may
215 be an indicator of anaerobic degradation of *Microcystis* biomass [43,44], which in turn
216 could contribute to nutrient recycling within the larger bloom community. Interestingly,
217 very few reads mapped to marker genes for IAA synthesis, indicated that exposure to
218 bacterial-derived IAA was limited in the S-10 system at the time of sampling
219 (Supplementary Table 1).

220 While these bacteria have been identified as constituents of *Microcystis* blooms, no
221 direct measurements of interactions between *Microcystis* and these genera have been
222 completed, other than potential algicidal activity of individual strains of *Streptomyces*
223 against *Microcystis* [5,45–48]. To identify potential genes indicative of interaction with
224 *Microcystis* during bloom conditions, we examined the transcriptomes of three model
225 strains of these bacteria that were among the highest abundances of “Best Hit”
226 annotations of the contigs via Ref-Seq in the control treatment at 24 hours (Fig. 5).
227 Potential interaction markers include genes involved in nitrogen and carbohydrate
228 utilization, oxidative stress response, amino acid metabolism and transport, and vitamin
229 synthesis. All three bacteria highly expressed genes involved in amino acid synthesis
230 and metabolism, as well as peptidases. These included genes for the synthesis of

231 tryptophan (*trpA, trpB, trpD, aroC*), aromatic amino acids (*ilvB, ilvC, ilvD, ilvN*),
232 methionine (*metK*), and cysteine (*ahcY*) (Fig. 5). Previous work in strains of
233 *Acidobacteria* isolated from Lake Erie also implicated amino acids and peptides as
234 potential chemical currency exchanged between *Microcystis* and the bacterial
235 constituents of its phycosphere microbiome[16]. Additional studies have identified
236 tryptophan as a key component of the *Microcystis* EPS, and it has been correlated with
237 increased *Microcystis* density, as well as biochemical oxygen demand (BOD)[49]. The
238 presence of tryptophan in the *Microcystis* EPS may be a product of its microbiome,
239 rather than *Microcystis* itself, given the elevated expression of genes associated with
240 tryptophan biosynthesis in the three representative bacterial transcriptomes (Fig. 5).
241 The growth of *Microcystis* was positively impacted by tryptophan supplementation (Fig.
242 1e) and it could serve as a critical source of nitrogen and even serves as a component
243 of a congener of microcystin[50].

244 Individually, the different strains examined appear to serve different supportive roles in
245 the phycosphere microbiome (Fig. 5). *C. ljungdahlii* DSM 13528 highly expressed (>
246 1000 TPM) a suite of genes involved in cyanocobalamin ($B_{12}$) biosynthesis (Fig. 5);
247 heterotrophic bacteria are well-known contributors to algal $B_{12}$ demand in both
248 freshwater and marine systems[9]. Elevated expression of genes involved in $B_{12}$
249 synthesis in *C. ljungdahlii* DSM 13528 has been associated with organoheterotrophy,
250 rather than lithoautotrophy[51], indicating they were likely consuming organic carbon
251 potentially derived from *Microcystis*.

252 Among the most notorious roles for heterotrophic bacterial partners in the phycosphere
253 is neutralizing reactive oxygen species. Best characterized in the *Prochlorococcus*-

254 *Alteromonas* system[15,52], there is substantial evidence for a similar relationship between
255 *Microcystis* and its phycosphere microbiome[14,16]. Super oxide disumutase was among
256 the most highly expressed genes for both *C. necator* H16 (*sodB*) and *S. avermitilis* MA-
257 4680 (*sodN*) (Fig. 5). This enzyme is a critical protectant against superoxide anion ($O_2^-$)
258 stress, which can inhibit key cellular processes including branched chain amino acid
259 synthesis and the TCA cycle[53]. Activity of this enzyme produces $H_2O_2$, which in turn
260 needs to be further neutralized through activity of catalases and peroxidredoxins, both
261 of which were highly expressed by *C. necator* H16 during bloom conditions (Fig. 5). As
262 an obligate anaerobe, the genome of *C. ljungdahlii* does not contain the machinery for
263 the neutralization of reactive oxygen and its contribution to this bloom community
264 function was negligible (Fig. 5).

265 Bacterial constituents of the phycosphere have been implicated in multiple stages of the
266 nitrogen cycle, and the idea that cyanobacteria interact with bacteria capable of provide
267 ammonium via nitrogen fixation has been established for several decades[54].
268 Heterotrophic bacteria have also been shown to act as a P bank for *Microcystis* during
269 variable P concentrations in culture[12]. In the S-10 bloom community, *C. necator* was the
270 primary bacterium responsible for N transport (*amt, urtA*) and metabolism (*nifH, ureC,*
271 *glnA, gltB*), while *S. avermitilis* appeared to play a dominant role in P transport
272 (*pstSABC*) and mineralization (*phoX, ugpQ*), while the role of *C. ljungdahlii* was minimal
273 for both (Fig. 5).

274 **Conclusions.** Due to the inherent nature of sequence data, results often take the form
275 of new hypotheses, rather than definitive conclusions. Here, we provide evidence that
276 exposure to IAA induces an antioxidant response in *Microcystis* during bloom

277 conditions. However, we did not find conclusive evidence for bacterial synthesis of IAA
278 during bloom conditions. We hypothesize that, as in the rhizosphere[55,56], bacterial
279 synthesis of IAA is dependent on the photobiont host development, and in this case, the
280 bloom was already extremely dense. Individual constituents and their functional role
281 within the *Microcystis* phycosphere are likely heavily dependent on the phase of bloom
282 development. In this study, we observed a striking impact of exposure to IAA and its
283 amino acid precursor, tryptophan, on *Microcystis* growth during dense bloom conditions.
284 Bacterial expression of IAA synthesis genes was, however, nearly undetectable in
285 metatranscriptome data from the different treatment conditions. Because IAA appears to
286 induce an antioxidant response in *Microcystis*, this function may be more critical during
287 early bloom development, when rapid population growth necessitates higher
288 photosynthetic rates and subsequently increased exposure to reactive oxygen species
289 like hydrogen peroxide. In this shallow pond, there was a clearly defined division of
290 labor between three representative bacterial strains, however, it is unlikely that these
291 specific genera fill this functional niche within freshwater cyanobacterial blooms
292 uniformly. Rather, it is likely that different species and genera fill various functional roles
293 that are dependent upon the stage of bloom development, physical characteristics of
294 individual lakes such as depth, latitude, or nutrient inputs, and the presence of
295 competing co-occurring cyanobacteria. Moving forward, it will be necessary to query all
296 of these individual parameters and their combined impacts on microbial community
297 dynamics to disentangle the role bacteria may have in freshwater ecosystem
298 conservation and bloom mitigation strategies.

299 **Methods**

300 **Sample Collection and Experimental Design.** Mesocosm experiments were
301 conducted in the experimental pond S-10 at Auburn University (32.669119, -85.508797)
302 from 09/29/2020 through 10/06/2020. Water from the *Microcystis*-dominated bloom was
303 enclosed in 1000 L mesocosms treated with 28 mM IAA, 48 μM tryptophan or a no
304 addition control in triplicate (Fig. 1a)[57,58]. Water samples were collected over a time
305 series at 0 h, 2 h, 12 h, 24 h, 48 h, and 7 days. 50 mL of water from the mesocosms
306 were filtered through Sterivex filters, treated with RNA*later*®, and kept on ice until frozen
307 at -80 °C prior to RNA extraction. Additional water samples were preserved in duplicate
308 with Lugol's iodine for cell counts. Cells were counted using a hemacytometer on a
309 bright-field microscope (Carl Zeiss Microscopy, Jena, Germany) at 40x magnification.
310 Environmental data was collected to measure weather conditions, temperature,
311 turbidity, dissolved oxygen, conductivity, pH, fluorescence, total phosphorus and
312 nitrogen, soluble reactive phosphorus, nitrate levels, total ammonia nitrogen, chlorophyll
313 a concentration, phycocyanin levels, toxin levels, and secondary metabolites MIB and
314 geosmin levels. Growth experiments were repeated in 4 L mesocosms with water
315 collected from a retention pond (38.43 N, -78.86 W) at James Madison University
316 (Harrisonburg, VA, USA) from 10/13/2021 through 10/19/2021. The October sample
317 collection is likely more representative of late, rather than peak, bloom conditions[59,60].
318 Water was incubated in sterile, acid washed 4 L cubitainers at 26 °C in a 12:12
319 light:dark cycle in triplicate, with concentrations and time points mimicking the S-10
320 pond incubations. Water samples were collected to measure cell density and
321 fluorescence at each time point. Non-axenic batch cultures of *Microcystis aeruginosa*
322 CCMP 3462 were added to CT media in triplicate under the same experimental

323 concentrations of IAA and tryptophan. Starting concentrations of the 175 mL cultures
324 were $10^6$ cells/mL were incubated at 26 °C in a 12:12 light:dark cycle. Cell counts and
325 fluorescence were measured at the same frequency as the field experiment and then
326 every 48 hours until stationary phase was reached. One-way ANOVA and Tukey's HSD
327 were used to determine significant differences in maximum growth rate (μ) for all growth
328 experiments.

329 **RNA Extraction and Sequencing.** Total RNA from the samples in the 0 h, 2 h, 12 h,
330 and 24 h time points was extracted using the Qiagen RNeasy PowerWater kit (Qiagen,
331 Hilden, Germany). Sterivex filters were opened according to Cruaud et al. and the
332 protocol was then followed according to the manufacturer's instructions, including
333 additional steps for removal of inhibitors and contaminating DNA[61]. After extraction,
334 additional DNA contamination was determined by PCR and gel electrophoresis using
335 16S primers 27f and 1492r[62]. DNA contamination was removed using a Qiagen DNase I
336 kit. Two rounds of DNase treatment were satisfactory to remove any contaminating
337 DNA. Quantification, sequencing, rRNA reduction, and library preparation were
338 performed by Azenta GeneWiz (South Plainfield, NJ). The rRNA reduction was
339 performed using the QIAGEN FastSelect rRNA kits for 5S, 16S, and 23S rRNA (Qiagen,
340 Hilden, Germany). The library was prepared using NEBNext Ultra II RNA Library
341 Preparation Kit for Illumina following the manufacturer's protocol (NEB, Ipswich, MD).
342 Enriched RNAs were fragmented at 95°C for 15 minutes. Then cDNA was synthesized
343 for first and second strand and enriched on a limited cycle PCR. The RNA integrity was
344 validated using the Agilent Tapestation 4200 (Agilent Technologies, Waltham, MA) as
345 well as qPCR (Kappa Biosystems, Wilmington, MA). The libraries were multiplexed and

346 clustered onto two lanes of a flowcell. The samples were then sequenced using paired-
347 end sequencing on an Illumina HiSeq platform (4000 or equivalent) according to
348 manufacturer's instructions.

349 **Metatranscriptome analysis.** To understand the impact that IAA exposure had on the
350 *Microcystis* transcriptome, the paired end sequence reads (fastq) were paired together
351 and aligned to the reference genome *Microcystis aeruginosa* NIES-843 (Kaneko et al.,
352 2007) in CLC genomics workbench as previously described[8,62,63]. Briefly, expression
353 values were calculated as Total per Million (TPM) with the minimum length fraction (0.9)
354 and similarity fraction (0.9) as the only exceptions to default parameter settings.
355 Differential expression was performed using the Differential expression for RNA-seq tool
356 in the program. Default parameters were used to determine differential expression in the
357 RNA-seq module using the Baggerly's t-test. Differential expression cutoffs were an
358 FDR corrected p-value of $< 0.05$ and Fold change of ±1.75. For the bacterial
359 transcriptomes, the reference genomes used were *Clostridium ljungdahlii* DSM 13528,
360 *Cupriavidus necator* H16, and *Streptomyces avermitilis* MA-4680 and length and
361 similarity fractions were set to 0.8 and 0.8, respectively. Values used for analysis were
362 from the 24 hr control samples. Contigs were assembled using the CLC Genomics
363 Workbench De novo assembly function with default parameters. Assembled contigs
364 were then exported for annotation and analysis using the MG-RAST metagenomic
365 server[64–66]. Abundance hits for the phylum, class, and order data files from MG-RAST
366 using Refseq annotation were transformed into percent abundance for analysis.
367 Functional characterization was performed in MG-RAST using the subsystems (SEED)
368 annotation analysis function. Figures were generated in Microsoft excel, Primer-e

369 (v.7.0.21), and GraphPad Prism. Sequences are available via the NCBI SRA (PRJNA
370 ##########) and contigs are available via MG-RAST (#########).

371 **References**


372 1. Bullerjahn, G. S. *et al.* Global solutions to regional problems: Collecting global
373 expertise to address the problem of harmful cyanobacterial blooms. A Lake Erie
374 case study. *Harmful Algae* **54**, 223–238 (2016).
375 2. Krausfeldt, L. E. *et al.* Urea is both a carbon and nitrogen source for *Microcystis*
376 *aeruginosa*: Tracking 13C incorporation at bloom pH conditions. *Front. Microbiol.* **10**,
377 1064 (2019).
378 3. Zepernick, B. N. *et al.* Elevated pH conditions associated with *Microcystis* spp.
379 blooms decrease viability of the cultured diatom *Fragilaria crotonensis* and natural
380 diatoms in Lake Erie. *Front. Microbiol.* **12**, 598736 (2021).
381 4. Anderson, D. M. Approaches to monitoring, control and management of harmful
382 algal blooms (HABs). *Ocean Coast. Manag.* **52**, 342–347 (2009).
383 5. Li, H., Xing, P. & Wu, Q. L. Characterization of the bacterial community composition
384 in a hypoxic zone induced by *Microcystis* blooms in Lake Taihu, China. *FEMS*
385 *Microbiol. Ecol.* **79**, 773–784 (2012).
386 6. Kenefick, S. L., Hrudey, S. E., Peterson, H. G. & Prepas, E. E. Toxin release from
387 *Microcystis aeruginosa* after chemical treatment. *Water Sci. Technol.* **27**, 433–440
388 (1993).
389 7. Qin, B. *et al.* A drinking water crisis in Lake Taihu, China: Linkage to climatic
390 variability and lake management. *Environ. Manage.* **45**, 105–112 (2010).

391 8. Steffen, M. M. *et al.* Ecophysiological examination of the Lake Erie
392 *Microcystis* bloom in 2014: Linkages between biology and the water supply
393 shutdown of Toledo, OH. *Environ. Sci. Technol.* **51**, 6745–6755 (2017).
394 9. Seymour, J. R., Amin, S. A., Raina, J.-B. & Stocker, R. Zooming in on the
395 phycosphere: The ecological interface for phytoplankton–bacteria relationships. *Nat.*
396 *Microbiol.* **2**, 17065 (2017).
397 10. Pound, H. L. *et al.* Environmental studies of cyanobacterial harmful algal blooms
398 should include interactions with the dynamic microbiome. *Environ. Sci. Technol.*
399 acs.est.1c04207 (2021) doi:10.1021/acs.est.1c04207.
400 11. Amin, S. A. *et al.* Interaction and signalling between a cosmopolitan phytoplankton
401 and associated bacteria. *Nature* **522**, 98–101 (2015).
402 12. Jiang, L. *et al.* Quantitative studies on phosphorus transference occuring between
403 *Microcystis aeruginosa* and its attached bacterium (*Pseudomonas* sp.).
404 *Hydrobiologia* **581**, 161–165 (2007).
405 13. Hoke, A. K. *et al.* Genomic signatures of Lake Erie bacteria suggest interaction in
406 the *Microcystis* phycosphere. *PLOS ONE* **16**, e0257017 (2021).
407 14. Smith, D. J. *et al.* Heterotrophic bacteria dominate catalase expression during
408 *Microcystis* blooms. *Appl. Environ. Microbiol.* **88**, e02544-21 (2022).
409 15. Morris, J. J., Johnson, Z. I., Szul, M. J., Keller, M. & Zinser, E. R. Dependence of the
410 cyanobacterium *Prochlorococcus* on hydrogen peroxide scavenging microbes for
411 growth at the ocean's surface. *PLoS ONE* **6**, e16805 (2011).
412 16. Smith, D. J., Kharbush, J. J., Kersten, R. D. & Dick, G. J. Uptake of phytoplankton-
413 derived carbon and cobalamins by novel *Acidobacteria* genera in *Microcystis*

414 blooms inferred from metagenomic and metatranscriptomic evidence. *Appl. Environ.*
415 *Microbiol.* **88**, e01803-21 (2022).
416 17. Lee, C. *et al.* Effects of an auxin-producing symbiotic bacterium on cell growth of the
417 microalga *Haematococcus pluvialis*: Elevation of cell density and prolongation of
418 exponential stage. *Algal Res.* **41**, 101547 (2019).
419 18. Chung, T.-Y., Kuo, C.-Y., Lin, W.-J., Wang, W.-L. & Chou, J.-Y. Indole-3-acetic-acid-
420 induced phenotypic plasticity in *Desmodesmus* algae. *Sci. Rep.* **8**, 10270 (2018).
421 19. Lupette, J. *et al. Marinobacter* dominates the bacterial community of the
422 *Ostreococcus tauri* phycosphere in culture. *Front. Microbiol.* **7**, 1414 (2016).
423 20. Sapp, M. *et al.* Species-specific bacterial communities in the phycosphere of
424 microalgae? *Microb. Ecol.* **53**, 683–699 (2007).
425 21. Harke, M. J. *et al.* A review of the global ecology, genomics, and biogeography of
426 the toxic cyanobacterium, *Microcystis* spp. *Harmful Algae Glob. Expans. Harmful*
427 *Cyanobacterial Blooms Divers. Ecol. Causes Controls* **54**, 4–20 (2016).
428 22. Cook, K. V. *et al.* The global *Microcystis* interactome. *Limnol. Oceanogr.* **65**, S194–
429 S207 (2020).
430 23. Lehman, P. W., Kurobe, T., Huynh, K., Lesmeister, S. & Teh, S. J. Covariance of
431 phytoplankton, bacteria, and zooplankton communities within *Microcystis* blooms in
432 San Francisco Estuary. *Front. Microbiol.* **12**, 632264 (2021).
433 24. Davenport, E. J. *et al.* Metatranscriptomic analyses of diel metabolic functions
434 during a *Microcystis* bloom in western Lake Erie (United States). *Front. Microbiol.*
435 **10**, 2081 (2019).

436 25. Martin, R. M. *et al.* Episodic decrease in temperature increases *mcy* gene
437 transcription and cellular microcystin in continuous cultures of *Microcystis*
438 *aeruginosa* PCC 7806. *Front. Microbiol.* **11**, 601864 (2020).
439 26. Harke, M. J., Davis, T. W., Watson, S. B. & Gobler, C. J. Nutrient-controlled niche
440 differentiation of western Lake Erie cyanobacterial populations revealed via
441 metatranscriptomic surveys. *Environ. Sci. Technol.* **50**, 604–615 (2016).
442 27. Leveau, J. H. J. & Gerards, S. Discovery of a bacterial gene cluster for catabolism of
443 the plant hormone indole 3-acetic acid: Genes in *Pseudomonas putida* 1290 for the
444 degradation of IAA. *FEMS Microbiol. Ecol.* **65**, 238–250 (2008).
445 28. Donoso, R. *et al.* Biochemical and genetic bases of indole-3-acetic acid (auxin
446 phytohormone) degradation by the plant-growth-promoting rhizobacterium
447 *Paraburkholderia phytofirmans* PsJN. *Appl. Environ. Microbiol.* **83**, e01991-16
448 (2017).
449 29. Harke, M. J., Jankowiak, J. G., Morrell, B. K. & Gobler, C. J. Transcriptomic
450 responses in the bloom-forming cyanobacterium *Microcystis* induced during
451 exposure to zooplankton. *Appl. Environ. Microbiol.* **83**, e02832-16 (2017).
452 30. Harke, M. J. & Gobler, C. J. Global transcriptional responses of the toxic
453 cyanobacterium, *Microcystis aeruginosa*, to nitrogen Stress, phosphorus stress, and
454 growth on organic matter. *PLoS ONE* **8**, e69834 (2013).
455 31. Pagnussat, L. A., Maroniche, G., Curatti, L. & Creus, C. Auxin-dependent alleviation
456 of oxidative stress and growth promotion of *Scenedesmus obliquus* C1S by
457 *Azospirillum brasilense*. *Algal Res.* **47**, 101839 (2020).

458 32. Kang, S.-M. *et al.* Indole-3-acetic-acid and ACC deaminase producing *Leclercia*
459 *adecarboxylata* MO1 improves *Solanum lycopersicum* L. growth and salinity stress
460 tolerance by endogenous secondary metabolites regulation. *BMC Microbiol.* **19**, 80
461 (2019).
462 33. Piotrowska-Niczyporuk, A. & Bajguz, A. The effect of natural and synthetic auxins on
463 the growth, metabolite content and antioxidant response of green alga *Chlorella*
464 *vulgaris* (Trebouxiophyceae). *Plant Growth Regul.* **73**, 57–66 (2014).
465 34. Piotrowska-Niczyporuk, A., Bajguz, A., Zambrzycka-Szelewa, E. & Bralska, M.
466 Exogenously applied auxins and cytokinins ameliorate lead toxicity by inducing
467 antioxidant defence system in green alga *Acutodesmus obliquus*. *Plant Physiol.*
468 *Biochem.* **132**, 535–546 (2018).
469 35. Kaneko, T. *et al.* Complete genomic structure of the bloom-forming toxic
470 cyanobacterium *Microcystis aeruginosa* NIES-843. *DNA Res.* **14**, 247–256 (2007).
471 36. Sánchez-Riego, A. M., López-Maury, L. & Florencio, F. J. Glutaredoxins are
472 essential for stress adaptation in the cyanobacterium *Synechocystis* sp. PCC 6803.
473 *Front. Plant Sci.* **4**, (2013).
474 37. Sánchez-Riego, A. M., Mata-Cabana, A., Galmozzi, C. V. & Florencio, F. J. NADPH-
475 Thioredoxin reductase C mediates the response to oxidative stress and
476 thermotolerance in the cyanobacterium *Anabaena* sp. PCC7120. *Front. Microbiol.* **7**,
477 (2016).
478 38. Wei, N., Hu, L., Song, L. & Gan, N. Microcystin-bound protein patterns in different
479 dultures of *Microcystis aeruginosa* and field samples. *Toxins* **8**, 293 (2016).

480 39. Alexova, R. *et al.* Specific global responses to N and Fe nutrition in toxic and non-
481 toxic *Microcystis aeruginosa*: Nutrient stress proteome of *Microcystis aeruginosa*.
482 *Environ. Microbiol.* **18**, 401–413 (2016).
483 40. Marsan, D., Place, A., Fucich, D. & Chen, F. Toxin-antitoxin systems in estuarine
484 *Synechococcus* strain CB0101 and their transcriptomic responses to environmental
485 stressors. *Front. Microbiol.* **8**, 1213 (2017).
486 41. Fei, Q., Gao, E.-B., Liu, B., Wei, Y. & Ning, D. A toxin-antitoxin system VapBC15
487 from *Synechocystis* sp. PCC 6803 shows distinct regulatory features. *Genes* **9**, 173
488 (2018).
489 42. Fucich, D. & Chen, F. Presence of toxin-antitoxin systems in picocyanobacteria and
490 their ecological implications. *ISME J.* **14**, 2843–2850 (2020).
491 43. Wang, S. *et al.* Variations of bacterial community during the decomposition of
492 *Microcystis* under different temperatures and biomass. *BMC Microbiol.* **19**, 207
493 (2019).
494 44. Wu, Y.-F., Xing, P., Liu, S. & Wu, Q. L. Enhanced microbial interactions and
495 deterministic successions during anoxic decomposition of *Microcystis* biomass in
496 lake sediment. *Front. Microbiol.* **10**, 2474 (2019).
497 45. Mou, X., Lu, X., Jacob, J., Sun, S. & Heath, R. Metagenomic identification of
498 bacterioplankton taxa and pathways involved in microcystin degradation in Lake
499 Erie. *PLoS One* **8**, e61890 (2013).
500 46. Zhao, D., Cao, X., Huang, R., Zeng, J. & Wu, Q. L. Variation of bacterial
501 communities in water and sediments during the decomposition of *Microcystis*
502 biomass. *PLOS ONE* **12**, e0176397 (2017).

503 47. Somdee, T., Sumalai, N. & Somdee, A. A novel actinomycete *Streptomyces*
504 *aurantiogriseus* with algicidal activity against the toxic cyanobacterium *Microcystis*
505 *aeruginosa*. *J. Appl. Phycol.* **25**, 1587–1594 (2013).
506 48. Zhang, B.-H. *et al.* Algicidal activity of *Streptomyces eurocidicus* JXJ-0089
507 metabolites and their effects on *Microcystis* physiology. *Appl. Environ. Microbiol.* **82**,
508 5132–5143 (2016).
509 49. Liu, L., Huang, Q., Zhang, Y., Qin, B. & Zhu, G. Excitation-emission matrix
510 fluorescence and parallel factor analyses of the effects of N and P nutrients on the
511 extracellular polymeric substances of *Microcystis aeruginosa*. *Limnologica* **63**, 18–
512 26 (2017).
513 50. Puddick, J. *et al.* Structural characterization of new microcystins containing
514 tryptophan and oxidized tryptophan residues. *Mar. Drugs* **11**, 3025–3045 (2013).
515 51. Tan, Y., Liu, J., Chen, X., Zheng, H. & Li, F. RNA-seq-based comparative
516 transcriptome analysis of the syngas-utilizing bacterium *Clostridium ljungdahlii* DSM
517 13528 grown autotrophically and heterotrophically. *Mol. Biosyst.* **9**, 2775 (2013).
518 52. Morris, J. J., Lenski, R. E. & Zinser, E. R. The Black Queen Hypothesis: Evolution of
519 dependencies through adaptive gene loss. *mBio* **3**, e00036-12 (2012).
520 53. Kim, Y. C., Miller, C. D. & Anderson, A. J. Superoxide dismutase activity in
521 *Pseudomonas putida* affects utilization of sugars and growth on root surfaces. *Appl.*
522 *Environ. Microbiol.* **66**, 1460–1467 (2000).
523 54. Paerl, H. W. & Gallucci, K. K. Role of chemotaxis in establishing a specific nitrogen-
524 fixing cyanobacterial-bacterial association. *Science* **227**, 647–649 (1985).

525 55. H., A., Z., Z., M., A. & A., K. Relationship between in vitro production of auxins by
526 rhizobacteria and their growth-promoting activities in *Brassica juncea* L. *Biol. Fertil.*
527 *Soils* **35**, 231–237 (2002).
528 56. Patten, C. L. & Glick, B. R. Role of *Pseudomonas putida* indoleacetic acid in
529 development of the host plant root system. *Appl. Environ. Microbiol.* **68**, 3795–3801
530 (2002).
531 57. Chen, X., Tang, Y., Sun, X., Zhang, X. & Xu, N. Comparative transcriptome analysis
532 reveals the promoting effects of IAA on biomass production and branching of
533 *Gracilariopsis lemaneiformis*. *Aquaculture* **548**, 737678 (2022).
534 58. Labeeuw, L. *et al.* Indole-3-acetic acid is produced by *Emiliania huxleyi* coccolith-
535 bearing cells and triggers a physiological response in bald cells. *Front. Microbiol.* **7**,
536 (2016).
537 59. Gobler, C. J., Davis, T. W., Coyne, K. J. & Boyer, G. L. Interactive influences of
538 nutrient loading, zooplankton grazing, and microcystin synthetase gene expression
539 on cyanobacterial bloom dynamics in a eutrophic New York lake. *Harmful Algae* **6**,
540 119–133 (2007).
541 60. Berry, M. A. *et al.* Cyanobacterial harmful algal blooms are a biological disturbance
542 to Western Lake Erie bacterial communities: Bacterial community ecology of
543 CHABs. *Environ. Microbiol.* **19**, 1149–1162 (2017).
544 61. Cruaud, P. *et al.* Open the SterivexTM casing: An easy and effective way to improve
545 DNA extraction yields. *Limnol. Oceanogr. Methods* **15**, 1015–1020 (2017).

546 62. Steffen, M. M. *et al.* Metatranscriptomic evidence for co-occurring top-down and
547 bottom-up controls on toxic cyanobacterial communities. *Appl. Environ. Microbiol.*
548 **81**, 3268–3276 (2015).
549 63. Krausfeldt, L. E. *et al.* Insight into the molecular mechanisms for microcystin
550 biodegradation in Lake Erie and Lake Taihu. *Front. Microbiol.* **10**, 2741 (2019).
551 64. Glass, E. M., Wilkening, J., Wilke, A., Antonopoulos, D. & Meyer, F. Using the
552 metagenomics RAST server (MG-RAST) for analyzing shotgun metagenomes. *Cold*
553 *Spring Harb. Protoc.* **2010**, pdb.prot5368 (2010).
554 65. Meyer, F. *et al.* The metagenomics RAST server – a public resource for the
555 automatic phylogenetic and functional analysis of metagenomes. *BMC*
556 *Bioinformatics* **9**, 1–8 (2008).
557 66. Aziz, R. K. *et al.* The RAST server: Rapid annotations using subsystems technology.
558 *BMC Genomics* **9**, 75 (2008).
559

560 **Acknowledgements**
561 MMS and MF were supported by NSF MCB-1716015. HRB was supported by NSF
562 DEB-1831106.

563 **Author Contributions**
564 M.M.S., M.I.G., H.R.B., M.F.G., and A.E.W. designed the experiments. M.F.G. and
565 A.E.W. conducted the mesocosm experiments. H.R.B. processed samples and
566 conducted culture experiments. M.M.S., H.R.B., and M.F. analyzed data. M.M.S.,
567 H.R.B., M.F.G., and A.E.W. interpreted the results and wrote the paper.

568 **Competing Interests Statement**

569 The authors declare no competing interests.

570 **Figure Legends**

571 Fig. 1: Bloom conditions during mesocosm sampling. Green represents the control
572 treatment, red represents the IAA treatment, and blue represents the tryptophan
573 treatment. a) Mesocosm setup and surface scum at onset of the incubation experiment.
574 b) Ratio of TN:TP during the 7 day time series. c) Concentration of photosynthetic
575 pigments across the time series; chlorophyll a is indicated by the solid lines and
576 phycocyanin is indicated by the dashed lines. Error bars represent standard deviation.
577 d) Microcystin concentration at the onset (0 hr) and conclusion (7 d) of the experiment.
578 Bars indicated mean of triplicated 1000 L enclosures. e) Change in average *Microcystis*
579 cell density (cells/mL) between each timepoint in the time series. ** indicates significant
580 difference ($p < 0.05$) between control and both IAA and tryptophan treatments. ¥
581 indicates significant difference ($p < 0.05$) between the IAA and tryptophan treatments. *
582 indicates significant difference ($p < 0.05$) between control and tryptophan treatments.
583 Significance was calculated using a t-test ($p < 0.05$). Environmental data are provided in
584 Supplementary Data File 1. Raw cell count data can be provided as an additional
585 supplementary data file upon request.

586 Fig. 2: Differential expression by *M. aeruginosa* in response to exposure to tryptophan
587 and IAA at 2, 12, and 24 hours. a) Differential expression of *M. aeruginosa* using the *M.*
588 *aeruginosa* NIES 843 genome at 2 (first column), 12 (second column), and 24 hours
589 (third column) for tryptophan (blue) and IAA (red). Gray points represent expression of
590 genes that were not significantly differentially expressed (FDR $p < 0.05$, FC ± 1.75).
591 Darker points are those genes that are significantly upregulated (FDR $p < 0.05$, FC +

592 1.75) compared to the control at each timepoint and lighter points are those genes that
593 are significantly downregulated (FDR $p < 0.05$, FC - 1.75) compared to the control at
594 each timepoint. All genes that were significantly different between control treatments at
595 each timepoint were excluded to ensure that only genes that were differentially
596 regulated due to exposure to IAA or tryptophan were considered. b) Expression values
597 (TPM) of all genes in the *mcy* microcystin toxin gene cassette. ● 0 hr, ■ 2 hr, ▲ 12 hr,
598 ◆ 24 hr. Green represents the control treatment, blue represents the tryptophan
599 treatment, and red represents the IAA treatment. Raw expression values as TPM are
600 provided as Supplementary Data File 2. Significance was calculated using a Baggerly's
601 t-test (FDR $p < 0.05$, FC ± 1.75).
602 Fig. 3: *Microcystis* expression patterns for genes in functional categories that were
603 differentially regulated due to IAA exposure. ● 0 hr, ■ 2 hr, ▲ 12 hr, ◆ 24 hr. Green
604 represents the control treatment, blue represents the tryptophan treatment, and red
605 represents the IAA treatment. a) Expression of genes (Log(x+1) TPM) involved in
606 nutrient transport and acquisition. b) Expression of genes (Log(x+1) TPM) involved in
607 growth and cell function. c) Expression of genes (Log(x+1) TPM) involved in stress
608 response. Gene names and locus tags correspond to the genome of *M. aeruginosa*
609 NIES 843.
610 Fig. 4: Impact of IAA and tryptophan exposure on the bloom bacterial community
611 composition. a) Percent abundance of short reads that recruited to the genomes of *M.*
612 *aeruginosa* NIES 843 (green), *C. necator* H16 (purple), *C. ljungdahlii* DSM 13528 (blue),
613 and *S. avermitilis* MA-4680 (yellow) in all samples grouped by time point. b) Total
614 microbial community makeup based on contig abundance, with duplicate libraries

615 averaged. Contigs were annotated using the Ref-Seq database with default parameters
616 in the MG-RAST pipeline. c) Abundance of the most predominant bacterial genera (>
617 1.5% contig abundance) in the phyla Cyanobacteria (top row), Proteobacteria (middle
618 row), and all other bacteria phyla (bottom row).
619 Fig. 5: Division of labor among key genera within the bloom population at 24 hours.
620 Percent abundance of the total TPM values for marker genes from five key functional
621 categories for *C. necator* H16 (purple) *C. ljungdahlii* DSM 13528 (blue), and *S.*
622 *avermitilis* MA-4680 (yellow): vitamin B12 synthesis (*cobA, cobB, cobQ*), ROS
623 neutralization (catalase, superoxide dismutase), amino acid synthesis and metabolism
624 (tryptophan, aromatic and branched chain amino acids, and methionine), phosphorus
625 transport and mineralization (*pstSABC*, alkaline phosphatase, *ugpQ*), and nitrogen
626 transport and metabolism (*nifH, narG, glnA, gltB, amt, urtA, ureC*). Raw data are
627 available in Supplementary Data File 4.

628 **Tables**

629 Table 1. Significant differences in maximum growth rate ($\mu$) when *Microcystis* is
630 exposed to IAA and its amino acid precursor tryptophan in field and culture populations.
631 One-way ANOVA and Tukey's HSD were used to determine significance ($p < 0.05$).

| | **S-10 $\mu$** | **S-10 P-value** | **CCMP 3462 $\mu$** | **CCMP 3462 P-value** | **Retention Pond $\mu$** | **Retention Pond P-value** |
|---|---|---|---|---|---|---|
| **Control** | 0.00415 | - | 0.00344 | - | 0.00760 | - |
| **Tryp** | 0.00652 | 0.001 | 0.00384 | 0.001 | 0.00765 | 0.001 |
| **IAA** | 0.00652 | 0.001 | 0.00374 | 0.001 | 0.00881 | 0.001 |

632
633
634
635
636
637

Fig. 1

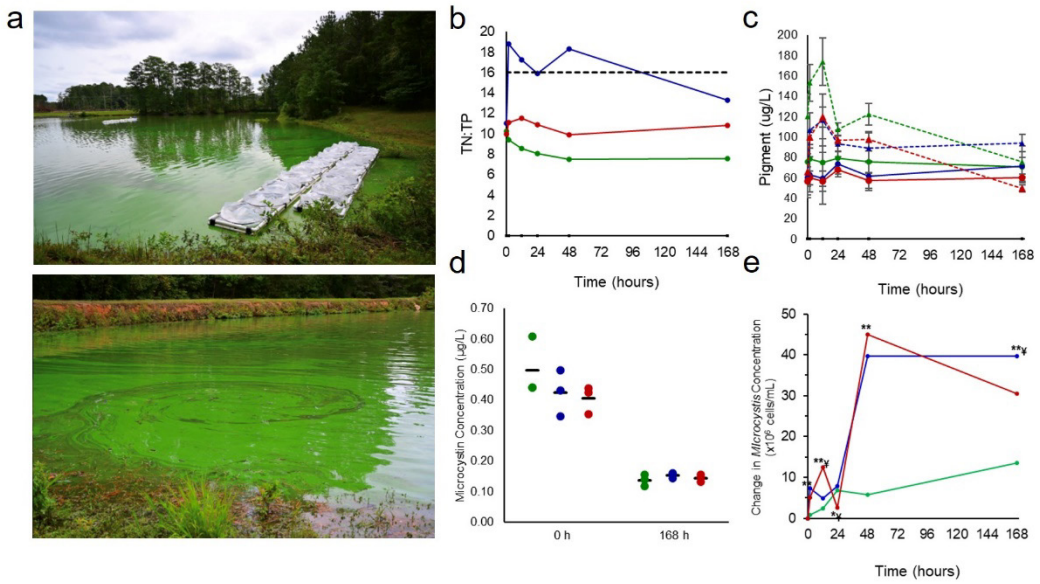


Fig. 2

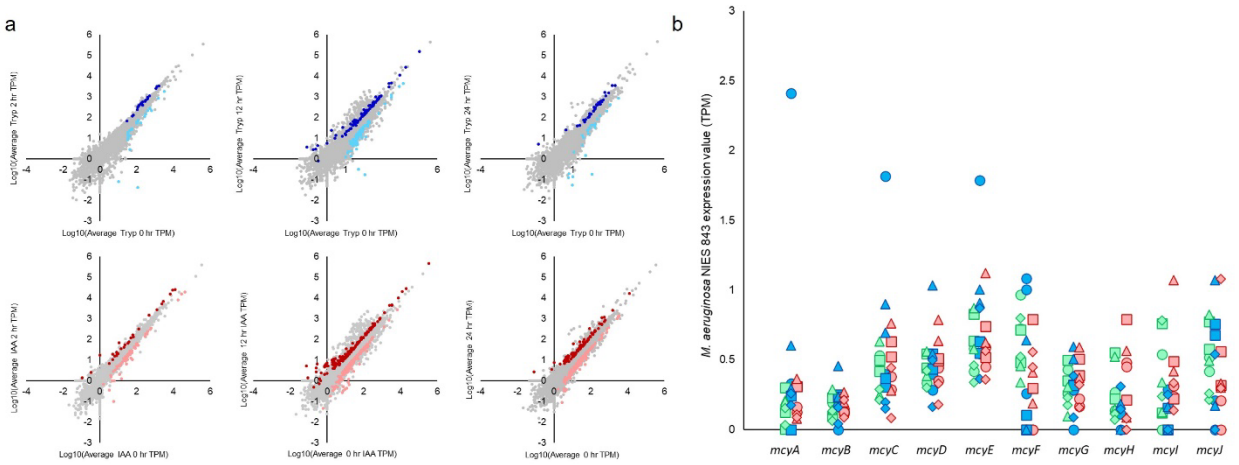


Fig. 3

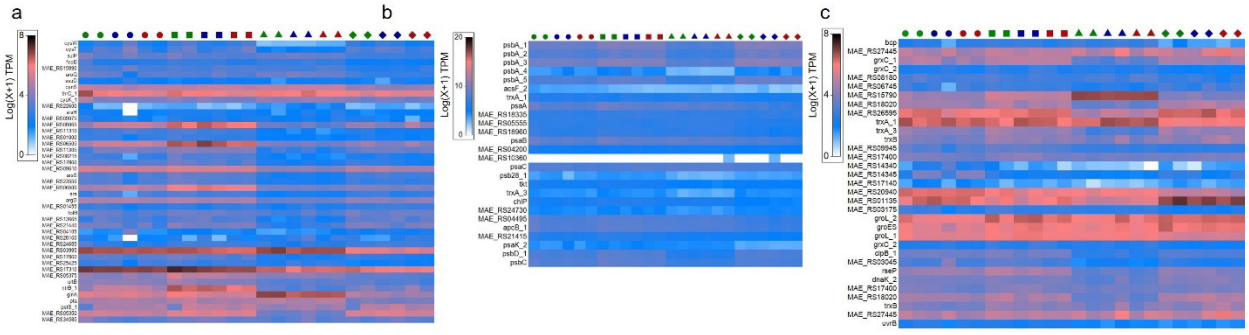

644 Fig. 4

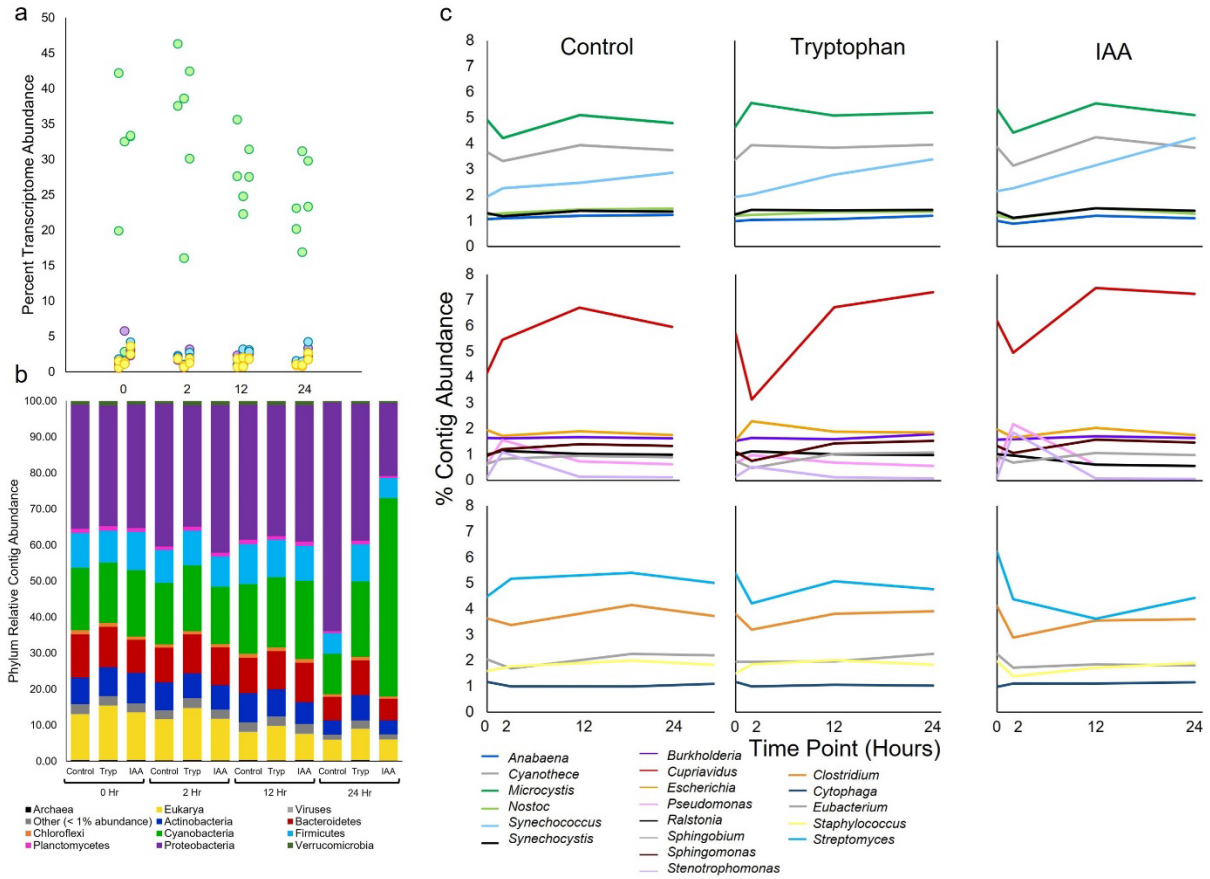


645

646 Fig. 5

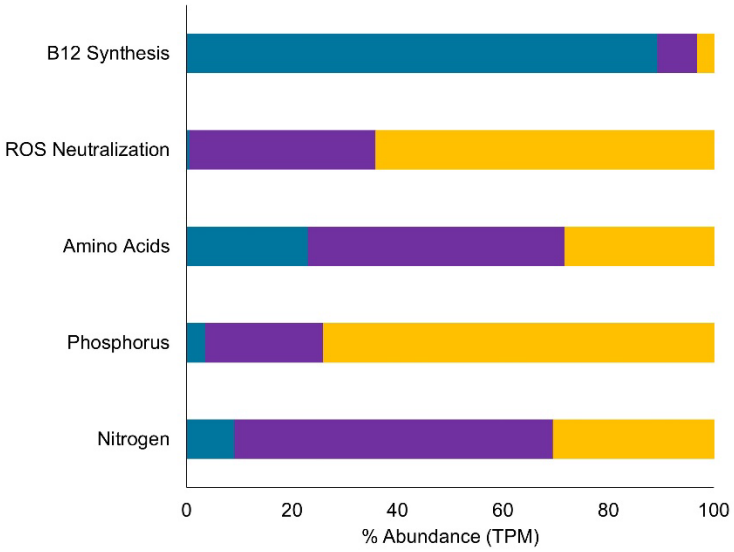


647